

Supporting Information

Toward a muon-specific electronic structure theory: Effective electronic Hartree-Fock equations for the muonic molecules

Milad Rayka¹, Mohammad Goli^{2,*} and Shant Shahbazian^{1,*}

*¹ Department of Physics and Department of Physical and Computational
Chemistry, Shahid Beheshti University, G. C., Evin, Tehran, Iran, 19839, P.O. Box
19395-4716.*

*² School of Nano Science, Institute for Research in Fundamental Sciences (IPM),
Tehran 19395-5531, Iran*

E-mails:

Mohammad Goli : mgoli2019@gmail.com

Shant Shahbazian: sh_shahbazian@sbu.ac.ir

* Corresponding authors

Table of contents

Pages 3-10: Deriving the EHF equations for [1s1p1d] muonic basis set and their computational implementation (containing **Tables S1 and S2** and **Figures S1-S3**).

Page 11: Table S3- The optimized [1s] nuclear exponents.

Page 12: Table S4- The optimized electronic exponents of [4s1p:1s] basis set.

Page 13: Table S5- The optimized muonic exponents of [4s1p:2s2p2d] basis set.

Page 14: Table S6- The optimized electronic exponents of [4s1p:2s2p2d] basis set.

Page 15: Table S7- Total energies computed with the optimized and averaged exponents using [6-311+g(d)/4s1p:1s] and [6-311+g(d)/4s1p:2s2p2d] basis sets. The energy differences between the optimized and averaged basis sets have been given in columns with the headline “Diff.” in milli-Hartrees. The two last columns contain the energy difference between the two averaged basis sets and between the two optimized basis sets in milli-Hartrees.

Page 16: Table S8- The distances between the banquet atoms and the central clamped nuclei computed with the optimized and averaged exponents using [6-311+g(d)/4s1p:1s] and [6-311+g(d)/4s1p:2s2p2d] basis sets. The distance differences between the optimized and averaged basis sets have been given in columns with the headline “Diff.” in Angstroms. The two last columns contain the distance difference between the two averaged basis sets and between the two optimized basis sets in Angstroms.

Page 17: Table S9- The angles between the two banquet atoms through the central clamped nuclei computed with the optimized and averaged exponents using [6-311+g(d)/4s1p:1s] and [6-311+g(d)/4s1p:2s2p2d] basis sets. The angle differences between the optimized and averaged basis sets have been given in columns with the headline “Diff.” in degrees. The two last columns contain the angle difference between the two averaged basis sets and between the two optimized basis sets in degrees.

Page 18: Figure S4- The difference in the mean inter-nuclear distances (of the quantum nucleus and the central atom distance) (a) and the difference in total energies (b) of the singly-substituted $X = \mu, H, D, T$ species relative to their clamped nucleus counterparts, computed at NEO-HF/[6-311++g(d,p)/4s1p:1s] and HF/6-311++g(d,p) levels, respectively.

Deriving the EHF equations for [1s1p1d] muonic basis set and their computational implementation

Previous computational experiences reveal that a combination of the s-, p- and d-type Cartesian gaussian functions suffices for a relatively accurate description of the nuclear spatial orbital at the NEO-HF level [S1]. Accordingly, a [1s1p1d] muonic basis set and a [4s1p] electronic basis set are used to expand the muonic spatial orbital and to describe the electronic distribution around the muon, respectively. A joint center, a *banquet* atom, at the z-axis is employed for all the muonic and the electronic basis functions, and the clamped carbon and nitrogen nuclei are placed at the same axis while the center of the coordinate system is fixed at the clamped carbon nucleus. In order to describe the electronic distribution around the clamped nuclei Pople-type 6-311+g(d) basis set is placed at the positions of the clamped nuclei [S2-S4]. For the muonic and corresponding electronic basis functions all parameters, i.e., the SCF linear coefficients, the exponents of the gaussian functions and the position of the joint center of the basis functions are optimized variationally during the NEO-HF calculation. In the process of the optimization of the exponents of the gaussian basis functions, the exponents of each type of gaussian function, e.g., *p*-type, are constrained to be the same for all members of the subset, e.g., p_x, p_y, p_z , and are denoted as $\alpha_s, \alpha_p, \alpha_d$ (the μ subscript is dropped hereafter for brevity). On the other hand, for the electronic basis sets centered on the clamped nuclei only the SCF coefficients are optimized, as is usual in the course of the conventional HF calculations [S5]. The geometry of the clamped nuclei is optimized using the analytical gradients of the total energy [S6], while for the optimization of the exponents of the basis functions a non-gradient optimization algorithm is used as described previously [S7-S10]. The mass of the muon was fixed at 206.768 in atomic units throughout the calculations and the whole NEO-HF calculations are also redone on hydrogen cyanide molecule where the proton is conceived as a quantum particle with a mass fixed at 1836 in atomic units.

Table S1 offers the variationally determined exponents and the SCF coefficients of the muonic and the protonic basis functions; from the original ten basis functions in [1s1p1d] basis set, only five basis functions namely, $s, p_z, d_{x^2}, d_{y^2}, d_{z^2}$, have non-zero SCF coefficients.

Table S1- The variationally optimized SCF coefficients and exponents of the muonic and the protonic basis functions derived from the NEO-HF calculations.

Type of basis functions	μCN		HCN	
	SCF coefficients	exponents	SCF coefficients	exponents
s	0.789	7.84	0.826	27.62
p_z	-0.206	5.51	-0.218	21.86
d_x²	0.143	5.94	0.104	22.73
d_y²	0.143		0.104	
d_z²	0.059		0.059	

The normalized muonic and protonic spatial orbitals are both linear combinations of these five basis functions:

$$\Psi_{\mu-sp d} = c_1\varphi_s + c_2\varphi_{p_z} + c_3\varphi_{d_{x^2}} + c_4\varphi_{d_{y^2}} + c_5\varphi_{d_{z^2}}, \Psi_{proton-sp d} = c'_1\varphi_s + c'_2\varphi_{p_z} + c'_3\varphi_{d_{x^2}} + c'_4\varphi_{d_{y^2}} + c'_5\varphi_{d_{z^2}}$$

$$\varphi_s = N_s \text{Exp}\left(-\alpha_s \left| \mathbf{r}_\mu - \mathbf{R}_c \right|^2\right) N_s = \left(\frac{8\alpha_s^3}{\pi^3}\right)^{\frac{1}{4}},$$

$$\varphi_{p_z} = N_p \bar{z}_{\mu c} \text{Exp}\left(-\alpha_p \left| \mathbf{r}_\mu - \mathbf{R}_c \right|^2\right) N_p = \left(\frac{128\alpha_p^5}{\pi^3}\right)^{1/4}, \bar{z}_{\mu c} = z_\mu - Z_c$$

$$\varphi_{d_{x^2}} = N_d \bar{x}_{\mu c}^2 \text{Exp}\left(-\alpha_d \left| \mathbf{r}_\mu - \mathbf{R}_c \right|^2\right) N_d = \left(\frac{2048\alpha_d^7}{9\pi^3}\right)^{1/4}, \bar{x}_{\mu c}^2 = (x_\mu - X_c)^2$$

$$\varphi_{d_{y^2}} = N_d \bar{y}_{\mu c}^2 \text{Exp}\left(-\alpha_d \left| \mathbf{r}_\mu - \mathbf{R}_c \right|^2\right) \bar{y}_{\mu c}^2 = (y_\mu - Y_c)^2$$

$$\varphi_{d_{z^2}} = N_d \bar{z}_{\mu c}^2 \text{Exp}\left(-\alpha_d \left| \mathbf{r}_\mu - \mathbf{R}_c \right|^2\right) \bar{z}_{\mu c}^2 = (z_\mu - Z_c)^2 \quad (\text{S1})$$

Figure S1 compares the one-particle densities, $\rho_\mu = \Psi_{\mu-sp d}^2$ and $\rho_{proton} = \Psi_{proton-sp d}^2$, and in line with the numerical data in Table S1 it is clear that the latter is much more concentrated than the former while the anisotropic nature of both distributions is evident from the offered counter maps.

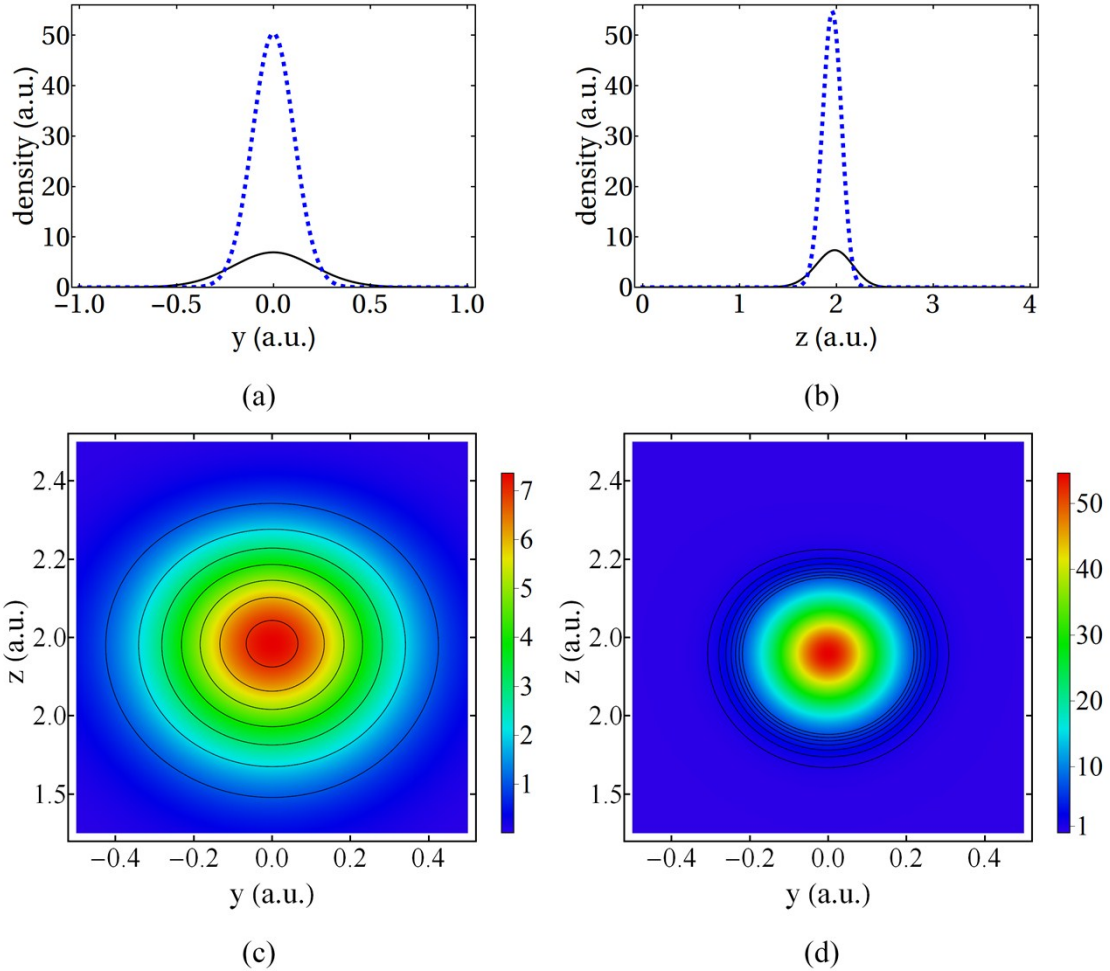


Figure S1- a) The one-particle protonic (dashed line) and muonic (full line) densities depicted along a y-axis, which goes through muon and is perpendicular to the z-axis. b) The same densities along the z-axis. The contour maps of the muonic (c) and the protonic (d) one-particle densities in μCN and HCN depicted at yz-plane, respectively (the contours lines are from $\rho = 1$ to 7, increased in integer steps). The clamped carbon nucleus is placed at the center of coordinate system while the clamped nitrogen nucleus and the banquet atom are placed at the negative and the positive sides of the z-axis, respectively.

Table S2 offers the total, the electronic, and the nuclear kinetic energies as well as the inter-nuclear distances computed at the NEO-HF level (the banquet atom is used as the third center).

Table S2- Some results of the NEO-HF calculations.

Energy	μCN	HCN
total	-92.79837	-92.86175
electronic kinetic	92.72631	92.81344
μ or proton kinetic	0.04216	0.01828
Distances		
C-N	1.128	1.127
Bq-C	1.132	1.082

The results demonstrate that upon the substitution of the proton with the muon, the latter's mean distribution and the kinetic energy increase relative to those of the former's. Also, the particle with the larger mass, because of its larger localization, is capable of localizing electrons more efficiently [S7], thus the electronic kinetic energy of the hydrogen cyanide molecule is larger than its muonic analog.

Taking into account that the NEO-HF calculation yields the anisotropy and anharmonicity of muon's vibrations using $\psi_{\mu-spd}$, it seems $\psi_{\mu-spd}$ to be a proper model to derive $V^{eff} = V_e^{eff} + U^{eff}$. Incorporating $\psi_{\mu-spd}$ into equation (2), in the main text, and after some mathematical manipulations, the corresponding effective electron-muon interaction, V_{e-spd}^{eff} , is derived:

$$\begin{aligned}
V_{e-spd}^{eff} &= \sum_i^{N_c} V_{spd}^{eff}(\mathbf{r}_i) \\
V_{spd}^{eff}(\mathbf{r}_i) &= -[c_{11}N_{ss} \left(\frac{2\pi}{\alpha_{ss}}\right) F_{0,ss}^i + c_{12}N_{sp} \left(\frac{4\pi}{\alpha_{sp}}\right) \bar{z}_{ic} F_{1,sp}^i + c_{22}N_{pp} \left(\frac{\pi}{\alpha_{pp}^2}\right) (F_{0,pp}^i - F_{1,pp}^i + 2\alpha_{pp} \bar{z}_{ic}^2 F_{2,pp}^i) \\
&\quad + N_{sd} \left(\frac{2\pi}{\alpha_{sd}^2}\right) \{ (c_{13} + c_{14} + c_{15})(F_{0,sd}^i - F_{1,sd}^i) + 2\alpha_{sd} (c_{13} \bar{x}_{ic}^2 + c_{14} \bar{y}_{ic}^2 + c_{15} \bar{z}_{ic}^2) F_{2,sd}^i \} \\
&\quad + N_{pd} \left(\frac{2\pi}{\alpha_{pd}^2}\right) \bar{z}_{ic} \{ (c_{23} + c_{24} + 3c_{25})(F_{1,pd}^i - F_{2,pd}^i) + 2\alpha_{pd} (c_{23} \bar{x}_{ic}^2 + c_{24} \bar{y}_{ic}^2 + c_{25} \bar{z}_{ic}^2) F_{3,pd}^i \} \\
&\quad + N_{dd} \left(\frac{\pi}{2\alpha_{dd}^3}\right) \{ 3(c_{33} + c_{44} + c_{55})(F_{0,dd}^i - 2F_{1,dd}^i + F_{2,dd}^i) + 12\alpha_{dd} (c_{33} \bar{x}_{ic}^2 + c_{44} \bar{y}_{ic}^2 + c_{55} \bar{z}_{ic}^2) \\
&\quad (F_{2,dd}^i - F_{3,dd}^i) + 4\alpha_{dd}^2 (c_3 \bar{x}_{ic}^2 + c_4 \bar{y}_{ic}^2 + c_5 \bar{z}_{ic}^2)^2 F_{4,dd}^i + 2(c_{34} + c_{35} + c_{45})(F_{0,dd}^i - 2F_{1,dd}^i + F_{2,dd}^i) \\
&\quad + 4\alpha_{dd} ((c_{34} + c_{35}) \bar{x}_{ic}^2 + (c_{34} + c_{45}) \bar{y}_{ic}^2 + (c_{35} + c_{45}) \bar{z}_{ic}^2) (F_{2,dd}^i - F_{3,dd}^i) \} \quad (S2)
\end{aligned}$$

In this expression $c_{tw} = c_t c_w$, $t, w = 1-5$ and $\alpha_{kl} = \alpha_k + \alpha_l$, $N_{kl} = N_k N_l$, $k, l = s, p, d$ while $\bar{x}_{ic}^n = (x_i - X_c)^n$, $n = 0-4$ (similarly for \bar{y}_{ic}^n and \bar{z}_{ic}^n), and $F_{n,kl}^i = \int_0^1 dg g^{2n} \text{Exp} \left(-(\alpha_k + \alpha_l) \left(\mathbf{r}_i - \mathbf{R}_c \right)^2 g^2 \right)$ are the Boys functions [S11]. It is straightforward to demonstrate that if $c_1 = 1$ and $c_2 = c_3 = c_4 = c_5 = 0$ then based on the fact that

$F_{0,ss}^i = \sqrt{\frac{\pi}{8\alpha_s}} \frac{\text{erf} \left[\sqrt{2\alpha_s} \left| \mathbf{r}_i - \mathbf{R}_c \right| \right]}{\left| \mathbf{r}_i - \mathbf{R}_c \right|}$ [S11], the effective electron-muon interaction reduces to that derived in equation (3) in the main text. Figure S2 depicts $V_{spd}^{eff}(\mathbf{r}_i)$ demonstrating that in contrast to V_{e-s}^{eff} , electrons experience a non-Coulombic anisotropic potential.

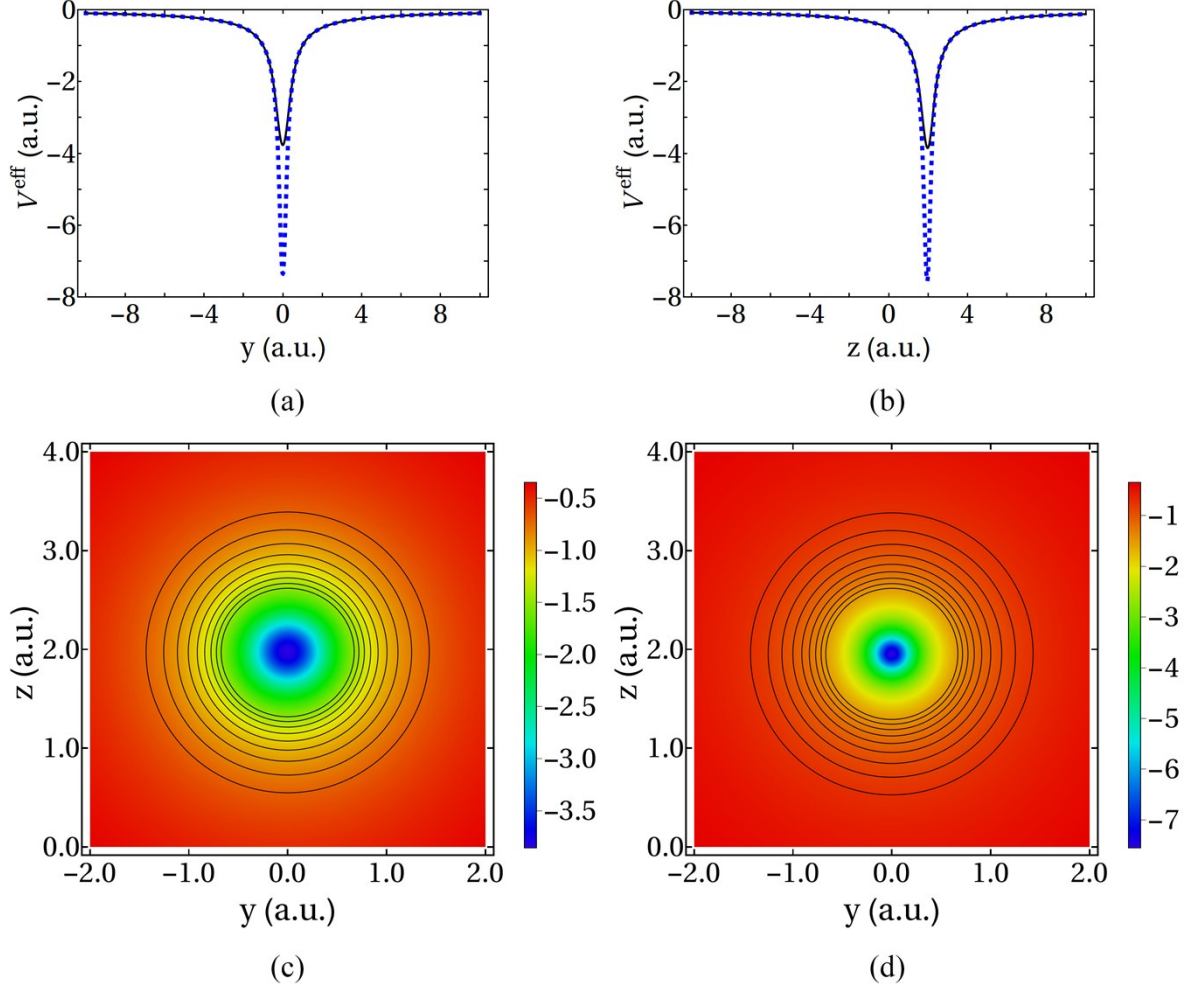


Figure S2- a) The effective muon-electron (full line) and proton-electron (dashed line) interaction potentials depicted along a y -axis, which goes through muon and is perpendicular to the z -axis. b) The same effective potentials along the z -axis. The contour maps of effective interaction potentials in μCN (c) and HCN (d) depicted at yz -plane (the contours lines are from $V_{spd}^{eff} = -0.7$ to -1.5 , decreased in -0.1 steps). The clamped carbon nucleus is placed at the center of coordinate system while the clamped nitrogen nucleus and the banquet atom are placed at the negative and the positive sides of the z -axis, respectively.

After some mathematical manipulations, the part of the effective potential, which appears because of the kinetic energy of the muon and the muon-clamped nuclei interaction, is derived:

$$\begin{aligned}
 U_{spd}^{eff} = & \frac{\hbar^2}{m_\mu} \left\{ c_{11} \left(\frac{3\alpha_s}{2} \right) + (c_{13} + c_{14} + c_{15}) \left(8\sqrt{\frac{2}{3}} \right) \left(\frac{(\alpha_s \alpha_d)^{\frac{7}{4}} (3\alpha_d - 2\alpha_s)}{(\alpha_s + \alpha_d)^{\frac{7}{2}}} \right) + c_{22} \left(\frac{5\alpha_p}{2} \right) \right. \\
 & \left. + (c_{33} + c_{44} + c_{55}) \left(\frac{13\alpha_d}{6} \right) - (c_{34} + c_{35} + c_{45}) \left(\frac{\alpha_d}{3} \right) \right\}
 \end{aligned}$$

$$\begin{aligned}
& + \sum_{\beta}^q Z_{\beta} [c_{11} N_{ss} \left(\frac{2\pi}{\alpha_{ss}} \right) F_{0,ss}^{\beta} + c_{12} N_{sp} \left(\frac{4\pi}{\alpha_{sp}} \right) \bar{z}_{\beta c} F_{1,sp}^{\beta} + c_{22} N_{pp} \left(\frac{\pi}{\alpha_{pp}^2} \right) (F_{0,pp}^{\beta} - F_{1,pp}^{\beta} + 2\alpha_{pp} \bar{z}_{\beta c}^2 F_{2,pp}^{\beta}) \\
& + N_{sd} \left(\frac{2\pi}{\alpha_{sd}^2} \right) \{ (c_{13} + c_{14} + c_{15})(F_{0,sd}^{\beta} - F_{1,sd}^{\beta}) + 2\alpha_{sd} (c_{13} \bar{x}_{\beta c}^2 + c_{14} \bar{y}_{\beta c}^2 + c_{15} \bar{z}_{\beta c}^2) F_{2,sd}^{\beta} \} \\
& + N_{pd} \left(\frac{2\pi}{\alpha_{pd}^2} \right) \bar{z}_{\beta c} \{ (c_{23} + c_{24} + 3c_{25})(F_{1,pd}^{\beta} - F_{2,pd}^{\beta}) + 2\alpha_{pd} (c_{23} \bar{x}_{\beta c}^2 + c_{24} \bar{y}_{\beta c}^2 + c_{25} \bar{z}_{\beta c}^2) F_{3,pd}^{\beta} \} \\
& + N_{dd} \left(\frac{\pi}{2\alpha_{dd}^3} \right) \{ 3(c_{33} + c_{44} + c_{55})(F_{0,dd}^{\beta} - 2F_{1,dd}^{\beta} + F_{2,dd}^{\beta}) + 12\alpha_{dd} (c_{33} \bar{x}_{\beta c}^2 + c_{44} \bar{y}_{\beta c}^2 + c_{55} \bar{z}_{\beta c}^2) \\
& (F_{2,dd}^{\beta} - F_{3,dd}^{\beta}) + 4\alpha_{dd}^2 (c_3 \bar{x}_{\beta c}^2 + c_4 \bar{y}_{\beta c}^2 + c_5 \bar{z}_{\beta c}^2)^2 F_{4,dd}^{\beta} + 2(c_{34} + c_{35} + c_{45})(F_{0,dd}^{\beta} - 2F_{1,dd}^{\beta} + F_{2,dd}^{\beta}) \\
& + 4\alpha_{dd} ((c_{34} + c_{35}) \bar{x}_{\beta c}^2 + (c_{34} + c_{45}) \bar{y}_{\beta c}^2 + (c_{35} + c_{45}) \bar{z}_{\beta c}^2) (F_{2,dd}^{\beta} - F_{3,dd}^{\beta}) \} \quad (S3)
\end{aligned}$$

In this expression $\bar{x}_{\beta c}^n = (X_{\beta} - X_c)^n$, $n = 0-4$ (similarly for $\bar{y}_{\beta c}^n$ and $\bar{z}_{\beta c}^n$) and $F_{n,kl}^{\beta} = \int_0^1 dg g^{2n} \text{Exp} \left(-(\alpha_k + \alpha_l) (\hat{R}_{\beta} - \hat{R}_c)^2 g^2 \right)$, while it is straightforward to demonstrate that if $c_1 = 1$ and $c_2 = c_3 = c_4 = c_5 = 0$ then U_{spd}^{eff} reduces to U_s^{eff} . Clearly, this effective potential, $V_{spd}^{eff} = V_{e-spd}^{eff} + U_{spd}^{eff}$, is much more complicated and more reliable than the effective potential in equation (3) in the main text, yielding a new set of the EHF equations:

$$\begin{aligned}
\hat{f}_{spd}^{eff}(\hat{r}_i) \psi_i(\hat{r}_i) &= \varepsilon_i \psi_i(\hat{r}_i) \quad i = 1, \dots, N_e/2 \\
\hat{f}_{spd}^{eff}(\hat{r}_i) &= \hat{h}(\hat{r}_i) + V_{spd}^{eff}(\hat{r}_i) + \sum_j^{N_e/2} [2\hat{J}_j(\hat{r}_i) - \hat{K}_j(\hat{r}_i)] \\
E_{total} &= E_{EHF-spd} + U_{spd}^{eff} + \sum_{\beta}^q \sum_{\gamma > \beta}^q \frac{Z_{\beta} Z_{\gamma}}{|\hat{R}_{\beta} - \hat{R}_{\gamma}|} \quad (S4)
\end{aligned}$$

The solution of the algebraic (Roothan-Hall-Hartree-Fock) version of equations (S4) using the basis set given in equation (S1) and simultaneous optimization of the muonic parameters namely, $\{c_i, i = 1-5\}$ and $\{\alpha_k, k = s, p, d\}$, as well as the geometry of the clamped nuclei, $\{\hat{R}_{\beta}\}$, is completely equivalent to the solution of the NEO-HF equations and simultaneous full optimization of the parameters of the muonic [1s1p1d] basis set and the geometry of the clamped nuclei. In the case of μCN , the results given in Tables S1 and S2 are recovered from equations (S4) apart from minor differences emerging from varied numerical accuracy of the corresponding computational procedures. In the case of the muonic parameters, it is evident

from Table S1 that: $c_1 > c_{i \neq 1}$, and if one starts from an initial guess where $c_1 = 1$ and $c_2 = c_3 = c_4 = c_5 = 0$, the starting effective electron-muon interaction, which is equal to that in equation (3) in the main text, varies marginally during the optimization procedure. As is also evident from Figure S3, the first term in the equation (S2), $N_{ss} \left(\frac{2\pi}{\alpha_{ss}} \right) F_{0,ss}^i$, is one order of magnitude larger than all the remaining terms in the electron-muon interaction and the other terms act more like perturbations modifying this dominant term.

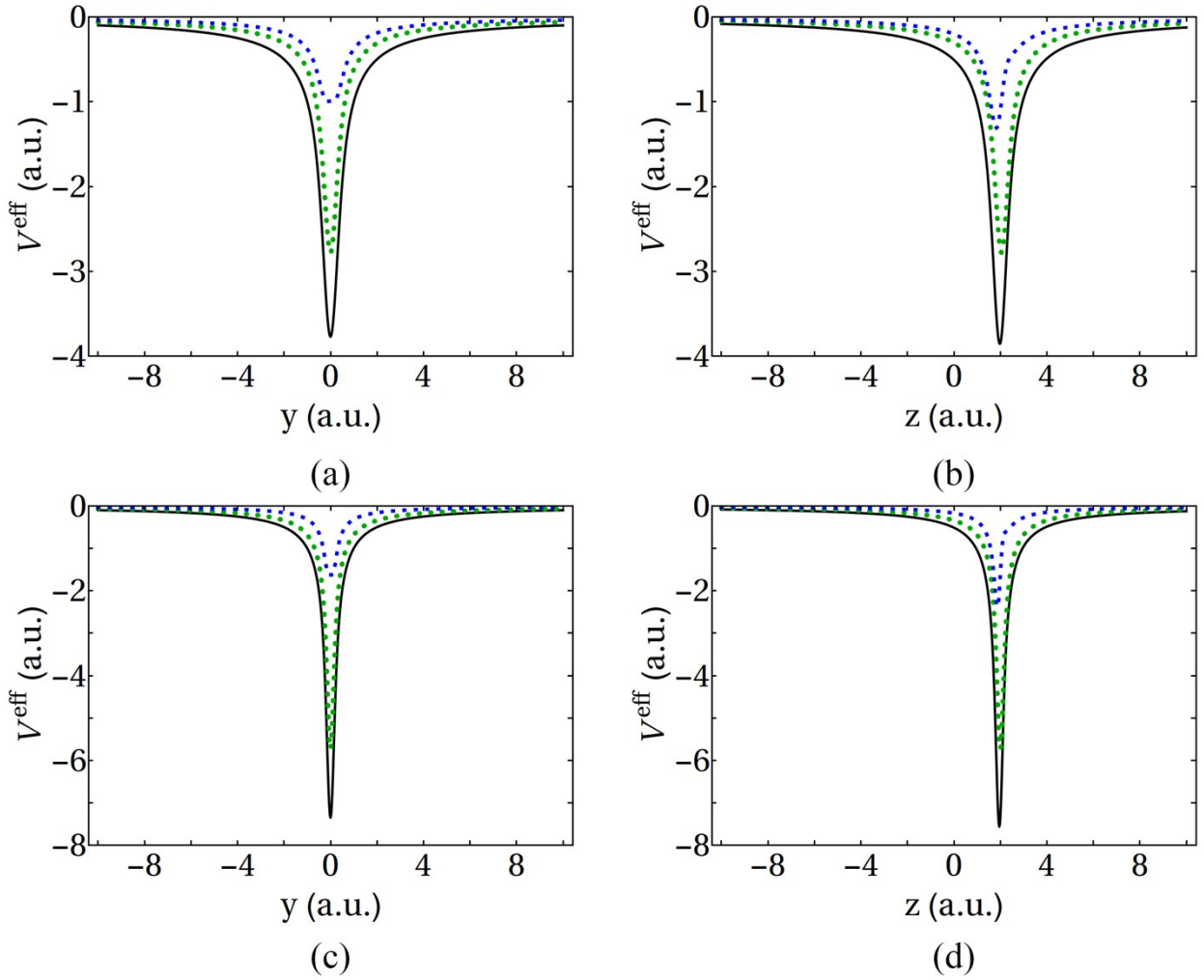


Figure S3- a) The components (the first term in equation (S2), $F_{0,ss}$, shown as green dotted, and all remaining terms, shown as blue dashed lines) and the total amount (full line) of the effective μ^+ -electron interaction potential in along a y-axis, which goes through muon and is perpendicular to the z-axis, and b) along z-axis. The same components and total amount of the effective proton-electron interaction potential along the y-axis, and (c) along the z-axis (d). The clamped carbon nucleus is placed at the center of coordinate system while the clamped nitrogen nucleus and the banquet atom are placed at the negative and the positive sides of the z-axis, respectively.

Further simplifications of the electron-muon potential are feasible based on this observation and one may derive a more compact electron-muon (or analogously muon-clamped nucleus) interaction potential simpler than equation (S2) (or equation (S3)) without a serious loss in accuracy as will be discussed in a future study.

References:

- [S1] S. P. Webb, T. Iordanov and S. Hammes-Schiffer, *J. Chem. Phys.* 117, 4106 (2002).
- [S2] W. J. Hehre, R. Ditchfield and J. A. Pople, *J. Chem. Phys.* 56, 2257 (1972).
- [S3] P. C. Hariharan and J. A. Pople, *Theoret. Chim. Acta* 28, 213 (1973).
- [S4] T. Clark, J. Chandrasekhar, G.W. Spitznagel and P. v. R. Schleyer, *J. Comp. Chem.* 4, 294 (1983).
- [S5] A. Szabo and N. S. Ostlund, *Modern Quantum Chemistry: Introduction to Advanced Electronic Structure Theory* (Dover Publications Inc., New York, 1996).
- [S6] T. Iordanov and S. Hammes-Schiffer, *J. Chem. Phys.* 118, 9489 (2003).
- [S7] M. Goli and Sh. Shahbazian, *Phys. Chem. Chem. Phys.* 16, 6602 (2014).
- [S8] M. Goli and Sh. Shahbazian, *Phys. Chem. Chem. Phys.* 17, 245 (2015).
- [S9] M. Goli and Sh. Shahbazian, *Phys. Chem. Chem. Phys.* 17, 7023 (2015).
- [S10] M. Goli and Sh. Shahbazian, *Chem. Eur. J.* 22, 2525 (2016).
- [S11] T. Helgaker, P. Jørgenson, J. Olsen, *Molecular Electronic-Structure Theory* (John Wiley & Sons, New York, 2000).

Table S3- The optimized [1s] nuclear exponents.

	X	Exponent	Molecule	X	Exponent
LiX	<i>T</i>	37.4538	NX₃	<i>T</i>	43.5257
	<i>D</i>	29.9147		<i>D</i>	34.7564
	<i>H</i>	20.1689		<i>H</i>	23.4532
	μ	5.2910		μ	6.2008
BeX₂			OX₂		
	<i>T</i>	40.6469		<i>T</i>	42.7551
	<i>D</i>	32.4777		<i>D</i>	34.1756
	<i>H</i>	21.9326		<i>H</i>	23.0908
	μ	5.8049	μ	6.1171	
BX₃			FX		
	<i>T</i>	42.8437		<i>T</i>	41.5458
	<i>D</i>	34.2321		<i>D</i>	33.1874
	<i>H</i>	23.1255		<i>H</i>	22.3832
	μ	6.1289	μ	5.8789	
CX₄	<i>T</i>	43.5861			
	<i>D</i>	34.8183			
	<i>H</i>	23.1255			
	μ	6.2158			
	X	Exponent	Molecule	X	Exponent
NaX	<i>T</i>	36.1904	PX₃	<i>T</i>	40.9091
	<i>D</i>	28.8930		<i>D</i>	32.6743
	<i>H</i>	19.4768		<i>H</i>	22.0381
	μ	5.0916		μ	5.7783
MgX₂			SX₂		
	<i>T</i>	38.2605		<i>T</i>	40.2265
	<i>D</i>	30.5693		<i>D</i>	32.1059
	<i>H</i>	20.6323		<i>H</i>	21.6323
	μ	5.4316	μ	5.6414	
AlX₃			CIX		
	<i>T</i>	40.0436		<i>T</i>	39.0553
	<i>D</i>	31.9967		<i>D</i>	31.1498
	<i>H</i>	21.6048		<i>H</i>	20.9424
	μ	5.7026	μ	5.4128	
SiX₄	<i>T</i>	41.0820			
	<i>D</i>	32.8258			
	<i>H</i>	22.1615			
	μ	5.8417			

Table S4- The optimized electronic exponents of [4s1p:1s] basis set.

	s	s	s	s	p		s	s	s	s	p
LiT	8.71	1.67	0.41	0.11	0.36	LiD	8.09	1.60	0.40	0.11	0.36
BeT₂	10.79	2.13	0.52	0.14	0.74	BeD₂	9.97	2.05	0.51	0.14	0.74
BT₃	12.94	2.65	0.67	0.18	1.00	BD₃	11.90	2.54	0.65	0.18	1.00
CT₄	14.02	2.94	0.77	0.22	1.15	CD₄	12.74	2.78	0.75	0.22	1.14
NT₃	14.47	3.06	0.82	0.26	0.79	ND₃	13.01	2.86	0.78	0.26	0.79
OT₂	9.87	1.86	0.51	0.15	0.70	OD₂	9.12	1.77	0.49	0.15	0.69
FT	10.34	2.00	0.58	0.16	0.84	FD	9.54	1.90	0.56	0.16	0.83
NaT	7.79	1.47	0.35	0.10	0.26	NaD	7.21	1.40	0.34	0.09	0.26
MgT₂	8.58	1.63	0.39	0.11	0.48	MgD₂	7.98	1.56	0.38	0.10	0.48
AlT₃	9.54	1.83	0.44	0.13	0.49	AlD₃	8.85	1.76	0.43	0.12	0.49
SiT₄	10.40	2.02	0.49	0.15	0.57	SiD₄	9.62	1.94	0.48	0.15	0.57
PT₃	10.80	2.13	0.53	0.17	0.56	PD₃	9.96	2.04	0.52	0.17	0.56
ST₂	11.24	2.24	0.56	0.18	0.58	SD₂	10.35	2.15	0.55	0.18	0.57
CIT	12.65	2.62	0.66	0.22	0.56	CID	11.67	2.52	0.65	0.22	0.56
	S	S	S	S	P		S	S	S	S	P
LiH	6.86	1.45	0.37	0.11	0.34	Liμ	3.54	0.97	0.29	0.09	0.31
BeH₂	8.53	1.88	0.49	0.13	0.74	Beμ₂	4.41	1.31	0.41	0.12	0.73
BH₃	10.16	2.35	0.63	0.18	0.98	Bμ₃	5.16	1.65	0.53	0.16	0.88
CH₄	10.55	2.49	0.71	0.21	1.10	Cμ₄	3.60	0.89	0.27	0.07	0.95
NH₃	10.49	2.46	0.72	0.24	0.77	Nμ₃	4.02	1.05	0.34	0.10	0.69
OH₂	7.89	1.63	0.47	0.14	0.69	Oμ₂	4.45	1.21	0.40	0.12	0.65
FH	8.16	1.73	0.53	0.15	0.83	Fμ	3.86	1.01	0.35	0.10	0.79
NaH	6.19	1.28	0.32	0.09	0.25	Naμ	3.24	0.86	0.25	0.08	0.23
MgH₂	6.90	1.45	0.36	0.10	0.48	Mgμ₂	3.73	1.04	0.30	0.09	0.46
AlH₃	7.63	1.62	0.41	0.12	0.48	Alμ₃	4.07	1.15	0.34	0.11	0.43
SiH₄	8.28	1.79	0.46	0.14	0.56	Siμ₄	4.43	1.28	0.39	0.13	0.52
PH₃	8.49	1.86	0.49	0.16	0.55	Pμ₃	4.27	1.24	0.39	0.15	0.47
SH₂	8.85	1.98	0.53	0.18	0.56	Sμ₂	4.55	1.36	0.44	0.16	0.49
ClH	9.88	2.33	0.62	0.22	0.55	Clμ	5.61	1.82	0.55	0.20	0.49

Table S5- The optimized muonic exponents of [4s1p:2s2p2d] basis set.

	s	s	p	p	d	d
Liμ	7.52	7.00	5.53	4.01	6.59	4.63
Beμ_2	8.28	6.34	4.43	3.79	6.57	4.75
Bμ_3	8.00	6.83	5.60	3.82	6.84	4.77
Cμ_4	8.93	7.66	6.01	4.11	7.18	4.98
Nμ_3	8.14	7.34	6.54	4.40	7.31	4.77
Oμ_2	9.58	5.81	6.94	4.49	7.68	4.64
Fμ	11.37	5.38	7.16	4.30	5.45	4.05
Naμ	7.56	7.08	5.63	3.95	6.22	4.42
Mgμ_2	7.72	7.00	5.97	4.41	6.50	4.60
Alμ_3	7.54	6.63	5.80	4.45	6.40	4.53
Siμ_4	7.87	6.75	5.66	4.23	6.56	4.64
Pμ_3	8.51	6.75	6.13	4.34	6.63	4.67
Sμ_2	7.44	6.75	6.35	4.29	6.66	4.46
Clμ	7.38	6.63	6.22	4.06	6.63	4.29

Table S6- The optimized electronic exponents of [4s1p:2s2p2d] basis set.

	s	s	s	s	p		s	s	s	s	p
LiT	8.74	1.67	0.41	0.11	0.29	LiD	8.06	1.60	0.40	0.11	0.29
BeT₂	10.80	2.14	0.52	0.14	0.68	BeD₂	10.47	2.21	0.57	0.16	0.12
BT₃	12.91	2.65	0.67	0.18	0.91	BD₃	11.89	2.54	0.65	0.18	0.90
CT₄	13.57	2.85	0.75	0.22	1.00	CD₄	12.19	2.66	0.72	0.22	0.98
NT₃	14.30	3.12	0.85	0.27	0.61	ND₃	12.91	2.93	0.82	0.26	0.60
OT₂	9.16	1.75	0.48	0.14	0.59	OD₂	8.59	1.70	0.47	0.14	0.59
FT	9.61	1.92	0.56	0.15	0.71	FD	8.94	1.85	0.55	0.15	0.71
NaT	7.84	1.47	0.35	0.10	0.23	NaD	7.25	1.41	0.34	0.09	0.22
MgT₂	8.61	1.63	0.39	0.11	0.45	MgD₂	8.57	1.73	0.43	0.11	0.14
AlT₃	10.18	2.03	0.51	0.15	0.08	AlD₃	9.40	1.94	0.49	0.15	0.08
SiT₄	10.37	2.02	0.49	0.15	0.51	SiD₄	9.61	1.94	0.48	0.15	0.51
PT₃	10.72	2.13	0.53	0.17	0.49	PD₃	9.90	2.04	0.52	0.17	0.48
ST₂	11.05	2.24	0.57	0.18	0.49	SD₂	10.20	2.15	0.56	0.18	0.49
ClT	12.18	2.62	0.67	0.22	0.47	ClD	11.24	2.52	0.66	0.22	0.47
	s	s	s	s	p		s	s	s	s	p
LiH	6.90	1.46	0.37	0.11	0.28	Liμ	3.54	0.96	0.29	0.09	0.23
BeH₂	8.84	2.01	0.54	0.15	0.12	Beμ₂	4.43	1.31	0.41	0.12	0.63
BH₃	10.13	2.34	0.63	0.18	0.87	Bμ₃	5.07	1.60	0.52	0.16	0.73
CH₄	10.30	2.41	0.69	0.21	0.94	Cμ₄	3.63	0.91	0.28	0.07	0.77
NH₃	10.35	2.50	0.75	0.25	0.59	Nμ₃	4.07	1.08	0.34	0.10	0.54
OH₂	7.50	1.58	0.45	0.13	0.58	Oμ₂	4.40	1.23	0.40	0.12	0.54
FH	7.79	1.73	0.53	0.15	0.70	Fμ	4.24	1.33	0.48	0.13	0.64
NaH	6.23	1.29	0.32	0.09	0.22	Naμ	3.28	0.87	0.25	0.08	0.19
MgH₂	7.38	1.59	0.41	0.11	0.14	Mgμ₂	3.77	1.04	0.30	0.09	0.41
AlH₃	8.05	1.78	0.47	0.14	0.08	Alμ₃	4.11	1.16	0.34	0.11	0.36
SiH₄	8.27	1.80	0.46	0.14	0.49	Siμ₄	4.43	1.28	0.38	0.13	0.43
PH₃	8.47	1.87	0.50	0.16	0.46	Pμ₃	4.30	1.26	0.40	0.15	0.38
SH₂	8.74	1.99	0.54	0.18	0.47	Sμ₂	4.30	1.31	0.44	0.16	0.38
ClH	6.31	1.96	0.58	0.21	0.49	Clμ	5.47	1.88	0.59	0.20	0.39

Table S7- Total energies computed with the optimized and averaged exponents using [6-311+g(d)/4s1p:1s] and [6-311+g(d)/4s1p:2s2p2d] basis sets. The energy differences between the optimized and averaged basis sets have been given in columns with the headline “Diff.” in milli-Hartrees. The two last columns contain the energy difference between the two averaged basis sets and between the two optimized basis sets in milli-Hartrees.

	1s	1s	1s	2s2p2d	2s2p2d	2s2p2d	Ave.	Opt.
	Opt.	Ave.	Diff.	Opt.	Ave.	Diff.	Diff.	Diff.
Liμ	-7.89187	-7.89149	0.38	-7.89199	-7.89178	0.21	0.29	0.12
Beμ_2	-15.56610	-15.56603	0.07	-15.56657	-15.56651	0.05	0.49	0.47
Bμ_3	-26.07424	-26.07322	1.02	-26.07575	-26.07532	0.43	2.09	1.51
Cμ_4	-39.77161	-39.76978	1.83	-39.77534	-39.77454	0.80	4.76	3.73
Nμ_3	-55.88687	-55.88607	0.80	-55.89250	-55.89232	0.17	6.25	5.63
Oμ_2	-75.83795	-75.83754	0.41	-75.84431	-75.84408	0.24	6.53	6.36
Fμ	-99.94933	-99.94847	0.86	-99.95406	-99.95334	0.72	4.87	4.73
Naμ	-162.28828	-162.28736	0.92	-162.28838	-162.28783	0.55	0.47	0.10
Mgμ_2	-200.53838	-200.53790	0.48	-200.53866	-200.53839	0.27	0.49	0.27
Alμ_3	-243.33596	-243.33570	0.25	-243.33676	-243.33656	0.20	0.86	0.80
Siμ_4	-290.84045	-290.84030	0.15	-290.84212	-290.84204	0.09	1.74	1.68
Pμ_3	-342.17069	-342.17018	0.50	-342.17293	-342.17243	0.50	2.24	2.24
Sμ_2	-398.50143	-398.50105	0.38	-398.50420	-398.50380	0.40	2.75	2.78
Clμ	-459.99891	-459.99857	0.34	-460.00098	-460.00073	0.26	2.16	2.08

Table S8- The distances between the banquet atoms and the central clamped nuclei computed with the optimized and averaged exponents using [6-311+g(d)/4s1p:1s] and [6-311+g(d)/4s1p:2s2p2d] basis sets. The distance differences between the optimized and averaged basis sets have been given in columns with the headline “Diff.” in Angstroms. The two last columns contain the distance difference between the two averaged basis sets and between the two optimized basis sets in Angstroms.

	1s	1s	1s	2s2p2d	2s2p2d	2s2p2d	Ave.	Opt.
	Opt.	Ave.	Diff.	Opt.	Ave.	Diff.	Diff.	Diff.
Liμ	1.697	1.688	0.009	1.683	1.686	-0.003	0.002	0.014
Beμ_2	1.415	1.416	-0.001	1.401	1.395	0.005	0.021	0.015
Bμ_3	1.267	1.273	-0.006	1.240	1.234	0.006	0.039	0.027
Cμ_4	1.155	1.161	-0.006	1.119	1.115	0.005	0.047	0.036
Nμ_3	1.068	1.073	-0.005	1.017	1.016	0.001	0.057	0.051
Oμ_2	1.006	1.010	-0.003	0.938	0.937	0.001	0.073	0.069
Fμ	0.964	0.966	-0.002	0.842	0.848	-0.006	0.118	0.122
Naμ	2.000	1.986	0.013	1.987	1.990	-0.002	-0.003	0.012
Mgμ_2	1.793	1.789	0.005	1.782	1.784	-0.002	0.005	0.012
Alμ_3	1.666	1.664	0.002	1.647	1.648	-0.001	0.016	0.020
Siμ_4	1.561	1.562	0.000	1.536	1.536	0.000	0.026	0.026
Pμ_3	1.492	1.491	0.001	1.453	1.456	-0.003	0.035	0.038
Sμ_2	1.411	1.408	0.003	1.353	1.359	-0.006	0.049	0.058
Clμ	1.349	1.344	0.005	1.276	1.283	-0.007	0.061	0.073

Table S9- The angles between the two banquet atoms through the central clamped nuclei computed with the optimized and averaged exponents using [6-311+g(d)/4s1p:1s] and [6-311+g(d)/4s1p:2s2p2d] basis sets. The angle differences between the optimized and averaged basis sets have been given in columns with the headline “Diff.” in degrees. The two last columns contain the angle difference between the two averaged basis sets and between the two optimized basis sets in degrees.

	1s	1s	1s	2s2p2d	2s2p2d	2s2p2d	Ave.	Opt.
	Opt.	Ave.	Diff.	Opt.	Ave.	Diff.	Diff.	Diff.
Nμ_3	109.1	108.5	0.6	109.1	108.8	0.3	-0.3	0.0
Oμ_2	107.6	107.3	0.3	107.4	107.4	-0.1	-0.1	0.2
Pμ_3	95.1	95.3	-0.2	95.0	95.1	0.0	0.2	0.1
Sμ_2	93.9	94.1	-0.2	93.9	93.7	0.1	0.4	0.1

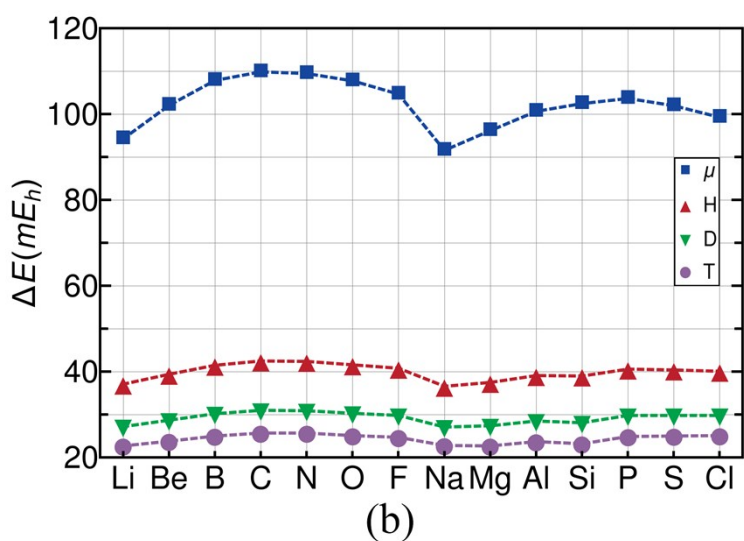
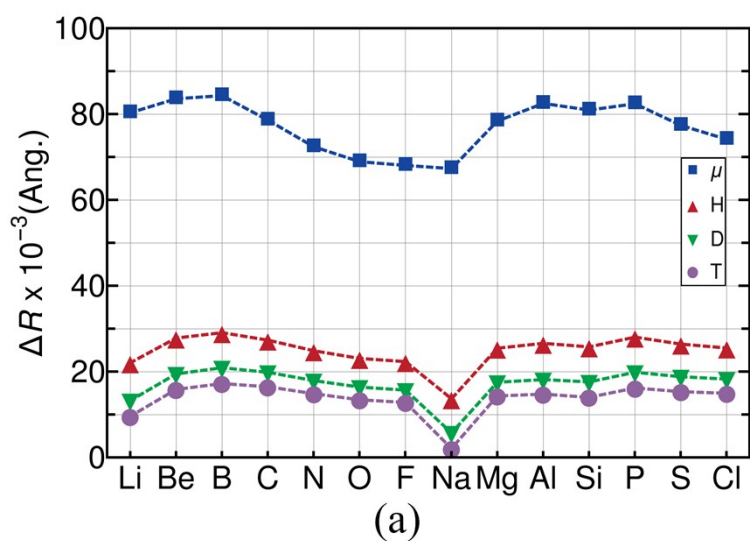


Figure S4- The difference in the mean inter-nuclear distances (of the quantum nucleus and the central atom distance) (a) and the difference in total energies (b) of the singly-substituted $X = \mu, H, D, T$ species relative to their clamped nucleus counterparts, computed at NEO-HF/[6-311++g(d,p)/4s1p:1s] and HF/6-311++g(d,p) levels, respectively.